Mathematical Modeling and Algorithm Application
ISSN: 3006-0842 | Vol. 7, No. 3, 2025

Active Control of Centrifugal Actuators for Enhanced Vehicle Lateral Stability: From Optimal Control of Measurable Disturbances to Robust Observation of Unmeasurable Disturbance

Jiatao Yu*

School of Mathematics, Foshan University, Foshan 528000, China
* **Corresponding author**: Jiatao Yu (Email: 15918037889@163.com)

Abstract: During vehicle operation, lateral disturbances such as crosswinds, uneven road surfaces, and load variations inevitably occur. In severe cases, these disturbances can compromise ride comfort, reduce handling stability, and even jeopardize driving safety. To enhance lateral stability under severe disturbance conditions, this study develops a vehicle-side active vibration suppression model using centrifugal actuators. The research focuses on two typical scenarios—"measurable disturbances" and "unmeasurable disturbances"—providing systematic modeling and control strategy development. The innovation lies in implementing a "control force reverse-engineering actuator angular displacement" method under measurable disturbance conditions, enabling actuators to achieve near-optimal vibration suppression even under constrained operating conditions and proposing an "observer + output feedback" actuator control architecture, which maintains robust vibration suppression performance even when interference forces remain unmeasurable. This study systematically investigates the lateral active vibration suppression strategy for centrifugal actuators through three dimensions: dynamic modeling, measurable disturbance optimal control, and unobservable disturbance state observation. The approach achieves comprehensive improvement in lateral vibration within the 20%–45% range, demonstrating the feasibility and engineering potential of centrifugal actuators in enhancing vehicle lateral stability.

Keywords: Centrifugal Actuator, Active Vibration Control, Vehicle Lateral Stability, Optimal Control, Disturbance Compensation.

1. Introduction

As equipment evolves toward higher speeds, larger sizes, and greater precision, structural vibration has become a critical factor limiting the performance and lifespan of engineering systems. Complex machinery such as vehicles, aircraft, and machine tools endure prolonged exposure to periodic or random disturbances during operation, which can trigger structural fatigue, loosening of connections, and even failure of critical components. These vibrations also amplify body sway, reduce handling stability, and compromise ride comfort. Given that traditional passive vibration damping devices struggle to meet performance requirements across multiple operating conditions, developing vibration suppression technologies capable of actively generating counter-control forces holds significant engineering importance [1].

The research of You Xiaoliang indicates that utilizing one drive motor to control frequency and phase, while employing another stepper motor to regulate the phase difference via a differential mechanism, is more suitable for engineering applications due to its lower requirement for phase accuracy [2]. Hao Zhenyang and others established precise models for the output force and load torque, and proposed a dual-motor parallel independent control strategy. Torque pulsations were effectively resolved through load feedforward optimization, thereby enhancing the system's robustness and disturbance rejection capability [3]. A simulation study was conducted on the servo control algorithm. The results demonstrate that the centrifugal actuator can complete the adjustment of output force amplitude, frequency, and phase within 0.5 seconds without any overshoot. Moreover, the servo control algorithm exhibits effective integration with the frequency-domain adaptive algorithm [4-6].

However, several issues remain now: the existing research has focused primarily on helicopter rotor systems, without addressing broader vibration control scenarios such as vehicle applications; the control algorithms are based on the assumption that disturbances are measurable or known, lacking robust handling of unmeasurable disturbances; and so on. This study introduces an observer-optimization control fusion framework that significantly addresses existing limitations. Regarding the narrow application scope and idealized disturbance handling in helicopter rotor vibration control, the framework expands the use of centrifugal actuators to lateral vehicle vibration suppression and employs an acceleration-based state observer to cope with unmeasurable disturbances, thereby enhancing robustness. To tackle the issue of simplistic control algorithms relying on full-state measurements, an integrated LQR optimal control method with observer feedback is adopted, achieving effective control using only acceleration sensors and compensating for the lack of state estimation. In response to the assumption of measurable disturbances, the study reconstructs system states to reduce vibration indices even under information constraints. Overall, the proposed innovative framework improves the applicability and engineering feasibility of centrifugal actuators in complex operational environments.

2. Model

2.1. Actuator angular displacement optimization model based on disturbance feedforward

When the lateral interference force time history is known, and the vehicle's lateral displacement, velocity, and acceleration can be measured, the optimization model addresses an active vibration suppression system for vehicles under measurable lateral disturbance forces, with the primary objective of minimizing lateral vibration metrics by optimizing the angular displacement trajectory of a centrifugal actuator. The vehicle is modeled as a single-degree-of-freedom mass-spring-damper system, in which the centrifugal actuator generates a controllable lateral inertial force through the rotation of an eccentric mass to counteract disturbance-induced vibrations. The core concept involves mapping the desired control force to a realizable angular displacement trajectory of the actuator, thereby optimizing the vibration response in the time domain. The Model schematic is shown in Figure 1.

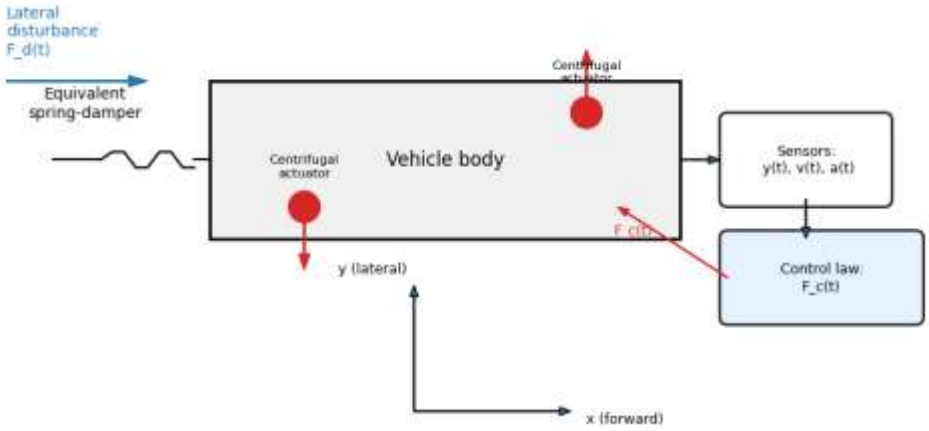


Figure 1. Model schematic

The optimization model consists of three basic elements, which are:

(1) The lateral equivalent force generated by the centrifugal actuator $F_c(t)$ is regarded as an adjustable "active control force", which acts on the vehicle body together with the external disturbance force $F_d(t)$; (2) The state vector is formed by $\dot{y}(t)$, $\ddot{y}(t)$ measuring the vehicle's lateral displacement y(t) and velocity, and a continuous-time state space model is established; (3) Taking the root mean square of the vehicle's lateral acceleration as the core metric, a quadratic performance index function is constructed. By $F_c(t)$ employing a linear quadratic regulator (LQR), the optimal feedback control law is derived to minimize vibrations of the virtual control force while complying with actuator constraints [7]; (4) According to the mechanical relation of the centrifugal actuator, the optimal control force $F_c(t)$ is mapped to the angular velocity $\omega(t)$ and angular displacement trajectory $\theta(t)$ of the eccentric block, and then the angular displacement curve satisfying the constraint is obtained, which realizes the control design goal.

The specific modeling process as follow:

The vehicle body is treated as concentrated mass $m_v = 2000$ kg, with lateral motion described by equivalent stiffness $k = 7.2252\times10^6$ N/m and damping $c = 3600$ N·s/m. The dynamics equation is:

$$m_v \ddot{y}(t) + c \dot{y}(t) + k y(t) = F_d(t) + F_c(t) \quad (1)$$

where y(t) is lateral displacement of the vehicle body relative to the track (or base), $\dot{y}(t)$ is lateral velocity, $\ddot{y}(t)$ is lateral acceleration, $F_c(t)$ is the centrifugal actuator synthesizes lateral equivalent control force and $F_d(t)$ is external lateral disturbance force. The actuator consists of four symmetrically arranged eccentric mass blocks, each with mass $m = 100$ kg and eccentric radius $r = 0.2$ m. By controlling angular velocity $\omega(t)$ and phase $\theta(t)$, the synthesized lateral force is :

$$F_c(t) = 4m_e r_e \omega^2(t) \sin\theta(t) \quad (2)$$

where m_e is the mass of a single eccentric mass and r_e is the eccentric radius. Physical constrains include maximum angular velocity $\omega_{max} = 100$ rad/s and maximum angular acceleration $\alpha_{max} = 5000$ rad/s^2. State variables are defined as $x_1(t) = y(t)$ and $x_2(t) = \dot{y}(t)$, then the state space form can be obtained from equation (1):

$$\dot{x_1}(t) = x_2(t), \quad (3)$$

$$\dot{x_2}(t) = -\frac{k_l}{m_v} x_1(t) - \frac{c_l}{m_v} x_2(t) + \frac{1}{m_v} F_d(t) + \frac{1}{m_v} F_c(t) \quad (4)$$

leading to the state equation:

$$\dot{x}(t) = A\, x(t) + B_d\, F_d(t) + B_c\, F_c(t) \quad (5)$$

where matrices A, B_d, B_c are derived from system parameters:

$$x(t) = \begin{bmatrix} x_1(t) \\ x_2(t) \end{bmatrix}, \quad A = \begin{bmatrix} 0 & 1 \\ -\frac{k_l}{m_v} & -\frac{c_l}{m_v} \end{bmatrix}, \quad B_d = B_c = \begin{bmatrix} 0 \\ \frac{1}{m_v} \end{bmatrix} \quad (6)$$

The vibration index is defined as the root mean square (RMS) of lateral acceleration:

$$I_y = \sqrt{\frac{1}{T}\int_0^T \ddot{y}^2(t)\, dt} \quad (7)$$

The goal is to minimize I_y by optimizing $F_c(t)$.

Optimal virtual control force design (based on LQR) : The control force $F_c(t)$ is virtual input u(t). A quadratic performance index is constructed:

$$J = \int_0^T (x^T(t) Q x(t) + r\, u^2(t))\, dt \quad (8)$$

By solving the algebraic Riccati equation, the optimal feedback control law is obtained:

$$u(t) = -K x(t) = -k_1 x_1(t) - k_2 x_2(t) \quad (9)$$

where weight matrices Q and r are tuned to align with

acceleration minimization.

The ideal control force u(t) is mapped to actuator angular displacement: The reference force $F_{ref}(t) = sat(|u(t)|, 0, F_{max})$, with $F_{max} = 4m_e r_e \omega_{max}^2$. Set $\sin\theta(t) = sgn(u(t))$ to ensure force direction opposes disturbances. Generate the reference angular velocity:

$$\omega_{ref}(t) = \sqrt{\frac{F_{ref}(t)}{4 m_e r_e}} \tag{10}$$

Smoothed via a first-order servo model:

$$\dot{\omega}(t) = sat\left(\frac{\omega_{ref}(t) - \omega(t)}{\tau}, \ -\alpha_{max}, \ \alpha_{max}\right) \tag{11}$$

where τ is the servo time constant, to satisfy acceleration constraints.

The fourth-order Runge-kutta method is used for numerical integration over 0-10 seconds, comparing two operational conditions: Actuator OFF: $F_c(t) = 0$, system responds only to disturbance; Actuator ON: Actuator follows the designed trajectory, generating active control force.

2.2. Extended state observer model based on acceleration measurements

This model is designed for active vibration suppression by integrating an observer with optimal control, specifically addressing scenarios where vehicles are subject to unknown lateral disturbances and only lateral acceleration can be measured via accelerometers. The core objective of the model is to generate compensatory control forces through centrifugal actuators to minimize the vehicle's lateral vibration index, thereby enhancing lateral stability and ride comfort under information-constrained conditions. By adopting an "observer + output feedback" structure, the model effectively addresses vibration suppression in partially observable systems. The specific modeling process as follow:

The vehicle is modeled as a single-degree-of-freedom mass-spring-damper system, considering only lateral translation displacement $y(t)$, while ignoring higher-order degrees of freedom like pitch and yaw. The dynamics equation is:

$$m_v \ddot{y}(t) + c_l \dot{y}(t) + k_l y(t) = F_d(t) + F_c(t) \tag{12}$$

where m_v is the equivalent mass of the car body, c_l is the equivalent damping of the car body, k_l is the equivalent stiffness of the car body, $F_d(t)$ is the external lateral disturbance force which is difficult to measure, $F_c(t)$ is the equivalent lateral control force generated by the centrifugal actuator are considered. Defining state variable $x_1(t) = y(t)$ and $x_2(t) = \dot{y}(t)$, the state equation is:

$$\dot{x}(t) = A x(t) + B u(t) + E d(t) \tag{13}$$

where $u(t) = F_c(t)$, $d(t) = F_d(t)$ and matrices A, B, E are derived from system parameters:

$$A = \begin{bmatrix} 0 & 1 \\ -\frac{k_l}{m_v} & -\frac{c_l}{m_v} \end{bmatrix}, \quad B = \begin{bmatrix} 0 \\ \frac{1}{m_v} \end{bmatrix}, \quad E = \begin{bmatrix} 0 \\ \frac{1}{m_v} \end{bmatrix} \tag{14}$$

Estimate displacement $y(t)$ and velocity $\dot{y}(t)$ in real-time using only acceleration measurements

$$a_y(t) = \ddot{y}(t) + n_a(t) \tag{15}$$

where $n_a(t)$ represents the measurement noise. According to Equation (13), the relationship between acceleration and state, control, and disturbance is

$$a_y(t) = -\frac{c_l}{m_v} \dot{y}(t) - \frac{k_l}{m_v} y(t) + \frac{1}{m_v} F_c(t) + \frac{1}{m_v} F_d(t) + n_a(t) \tag{16}$$

From Equation (17), the acceleration measurement is written as the output equation

$$z(t) = a_y(t) = C_a x(t) + D_a u(t) + w(t) \tag{17}$$

where

$$C_a = \begin{bmatrix} -\frac{k_l}{m_v} & -\frac{c_l}{m_v} \end{bmatrix}, \quad D_a = \frac{1}{m_v} \tag{18}$$

and $w(t) = \frac{1}{m_v} d(t) + n_a(t)$ (A, B, C_a, D_a) represents the combined interference and measurement noise. The Luenberger observer structure:

$$\dot{\hat{x}}(t) = A \hat{x}(t) + B u(t) + L (z(t) - \hat{z}(t)) \tag{19}$$

where $\hat{x}(t)$ is the estimated displacement and velocity of the vehicle body by the state observer, $\hat{z}(t) = C_a \hat{x}(t) + D_a u(t)$ is the acceleration estimate derived from the estimated state and $L \in R^{2\times1}$ serves as the observer gain vector via pole placement or Kalman filtering to ensure error convergence [8]. Control goal is to minimize the lateral vibration index:

$$I_y = \sqrt{\frac{1}{T} \int_0^T a_{\dot{y}}^2(t)\, dt} \tag{20}$$

where $[0, T]$ is the simulation time interval. Based on the estimated state $\hat{x}(t)$, the control force is a computed as $u(t) = -K \hat{x}(t)$, where feedback gain K is derived from the Riccati equation [9]. Weight matrices Q and R penalize state deviations and control effort. The controller and observer are designed independently, but closed-loop stability is ensured by the eigenvalues of $A - BK$ and $A - LC_a$ [10]. According to (2), the centrifugal actuator generates equivalent lateral force through symmetric eccentrics masses $F_c(t) = 4 m_e r_e \omega^2(t) \sin\theta(t)$. Angular velocity $|\omega(t)| \le \omega_{max} = 100$ rad/s, angular acceleration $|\dot{\omega}(t)| \le \alpha_{max} = 5000$ rad/s^2. Force direction is set by $\sin\theta(t) = sgn(u(t))$. Angular velocity is computed as

$$\omega(t) = \sqrt{\frac{|u(t)|}{4 m_e r_e}} \tag{21}$$

with a first-order filter for smoothness:

$$\tau_\omega \dot{\omega}_d(t) + \omega_d(t) = \sqrt{\frac{|u(t)|}{4 m_e r_e}} \tag{22}$$

where τ_ω is the equivalent time constant, $\omega_d(t)$ is the desired angular velocity.

3. Results and analysis

The data for this study was obtained from https://www.mojinghub.com/competitions.

3.1. Results and analysis of Actuator angular displacement optimization model

This section builds upon the lateral dynamics model of the vehicle body and the centrifugal actuator control model established in the previous section. Using the lateral disturbance force time series from data as input, we obtain the body's response under two operating conditions— "actuator inactive" and "actuator active" —through numerical integration. During computation, we establish a system of equations combining the lateral vibration equation with displacement-velocity feedback control law. By applying the fourth-order Runge-Kutta method for step-by-step integration from 0 to 10 seconds, we derive time series of lateral displacement, lateral velocity, and lateral acceleration. The calculated ideal control force is then transformed into actuator angular velocity and angular displacement curves through centrifugal force-angular velocity and angular displacement constraints, verifying compliance with maximum rotational

speed limits. Finally, the lateral vibration index is quantitatively assessed using the root mean square (RMS) definition based on lateral acceleration response, providing a metric for evaluating active control effectiveness.

The Comparison of Lateral Displacement Time Course is shown in Figure 2.

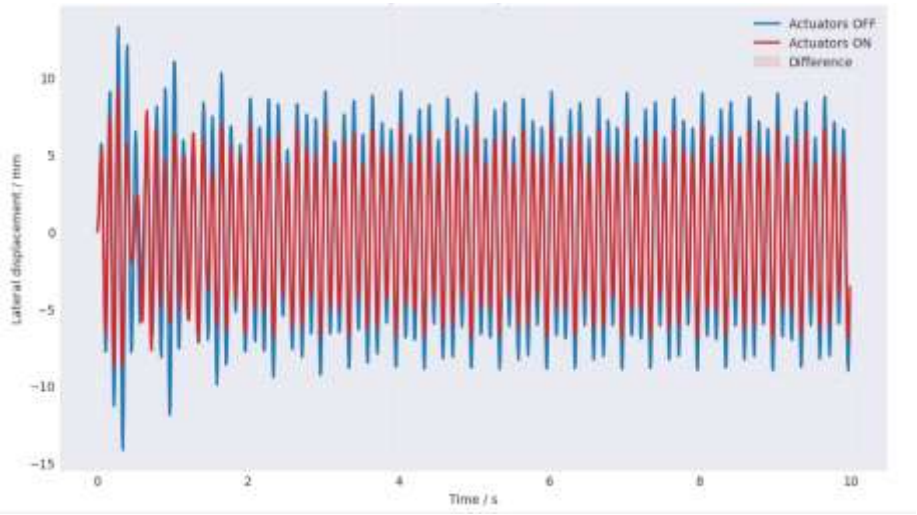


Figure 2. Comparison of Lateral Displacement Time Course

The Comparison of Lateral Displacement Time Course diagrams reveals that when the actuator is inactive, the vehicle body exhibits distinct periodic vibrations under interference, with peak displacement reaching approximately 14.16 mm. The vibration envelope shows gradual attenuation, maintaining substantial amplitude throughout the 0-10 second period. Upon activation of the centrifugal actuator, the displacement curve demonstrates marked envelope contraction, reducing peak displacement to 9.19 mm (35% decrease). Particularly during the initial 0-2 second vibration phase, active control effectively suppresses transient responses induced by interference, enabling the lateral displacement to rapidly approach zero. In the subsequent quasi-steady state phase, the amplitude under ON operation remains consistently lower than OFF conditions, demonstrating that the feedback control system with centrifugal actuators consistently reduces lateral body sway across the entire time-domain.

The Phase Plane Diagram (Displacement-Velocity Trajectory) is shown in Figure 3.

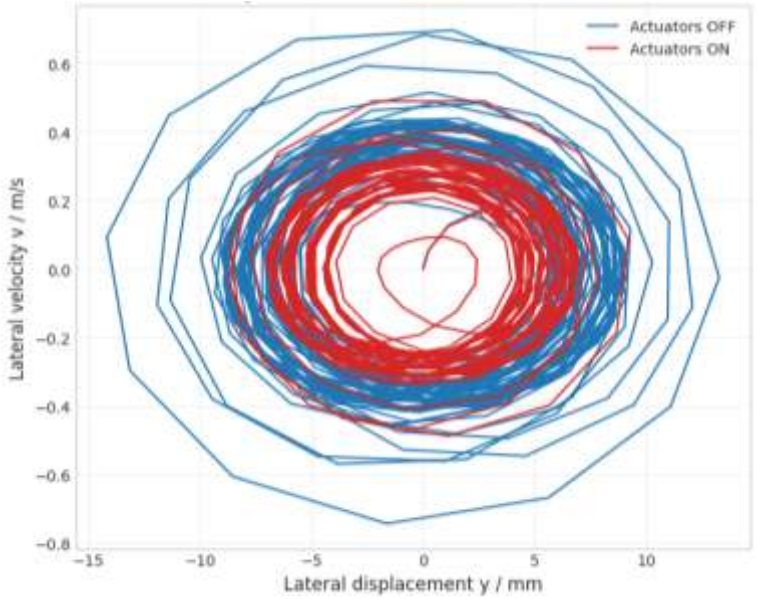


Figure 3. Phase Plane Diagram (Displacement-Velocity Trajectory)

The Phase Plane Diagram (Displacement-Velocity Trajectory) reveals that under inactive conditions, the trajectory forms a closed spiral curve with large radius, indicating significant energy circulation and relatively weak damping in the system. When the centrifugal actuator is activated, the trajectory contracts toward the origin, forming an elliptical path with smaller radius and higher concentration. This demonstrates a marked reduction in total system energy, substantial enhancement of equivalent damping, and accelerated dissipation of lateral vehicle vibrations.

3.2. Results and analysis of Extended state observer model

Given only lateral acceleration data, this section utilizes the previously established lateral vibration state-space model to reconstruct vehicle displacement and velocity through an acceleration output observer. The desired equivalent lateral control force is then calculated using the output feedback control law and implemented via the angular velocity and phase of a centrifugal actuator. For numerical simulation, the lateral disturbance force specified in data is applied as input. Time-domain simulations are conducted over the 0-10 second interval under two operational conditions: "centrifugal actuator deactivated (OFF)" and "observer + active output feedback control (ON)". The resulting lateral displacement, velocity, and acceleration responses are analyzed to calculate the lateral vibration index and related evaluation metrics. The Comparison of Transverse Vibration Index is shown in Figure 4.

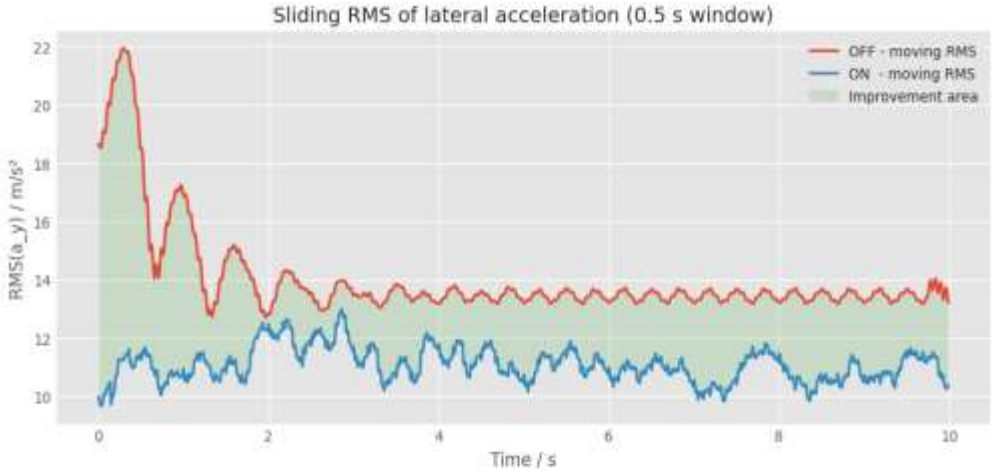


Figure 4. Comparison of Transverse Vibration Index

The Comparison of Transverse Vibration Index more intuitively demonstrates the improvement in overall vibration levels. Using the I_y root mean square value of lateral acceleration within 0-10 seconds as the vibration index, the uncontrolled condition showed approximately 14.12 m/s^2, while active control reduced it to about 11.08 m/s^2, representing an overall decrease of 21.54%. The local RMS calculated with a 0.5-second sliding window indicates that, throughout the time domain, the active control RMS curve consistently remains below the uncontrolled curve. The green shaded area between them represents the vibration energy "squeezed out" by active control, demonstrating that this strategy not only reduces peak acceleration but also continuously suppresses lateral vibration intensity throughout the operation.

The Cumulative Acceleration Energy Curve is shown in Figure 5.

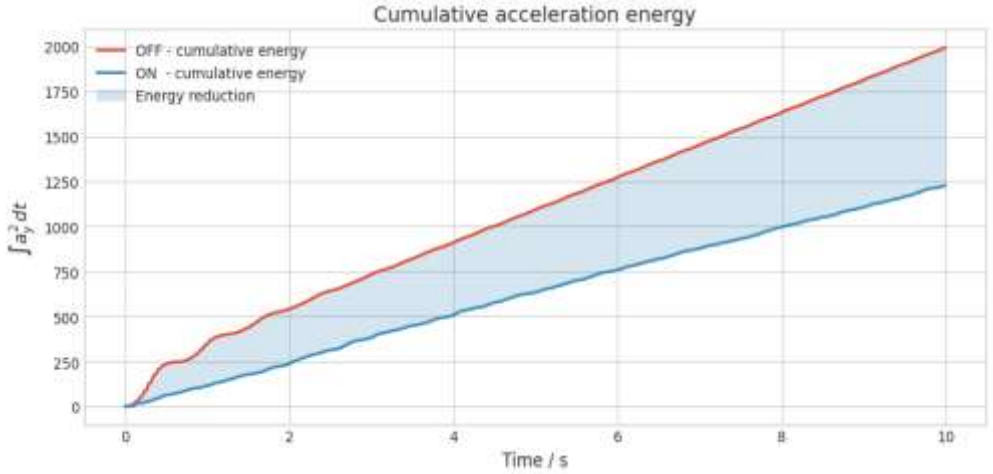


Figure 5. Cumulative Acceleration Energy Curve

From the perspective of vibration energy analysis, the Cumulative Acceleration Energy Curve provides a long-term effectiveness evaluation. Over time, the uncontrolled condition's energy curve shows a nearly linear increase, reaching approximately 2000 (unit: acceleration squared multiplied by time) after 10 seconds. In contrast, the active control condition demonstrates a significantly smoother curve, peaking at around 1250 and reducing cumulative energy by over one-third. The blue-filled area between the two curves represents the "excess vibration energy" absorbed or offset by the centrifugal actuator. This indicates that the observer + output feedback system not only improves transient response

but also effectively suppresses lateral vibration energy accumulation throughout the operational cycle, thereby reducing structural fatigue damage and enhancing ride comfort.

4. Conclusions and outlooks

This study proposes systematic control schemes for centrifugal actuators in both information-sufficient and information-constrained scenarios. Using LQR and force mapping, optimal disturbance rejection under measurable disturbances was achieved, while an observer was innovatively introduced to address unknown disturbances. Both approaches significantly reduced the vibration index, demonstrating the potential of centrifugal actuators in vehicle engineering. These methods can be extended to other vibration control domains (for example, lateral stability control of autonomous vehicles under limited sensor conditions and vibration suppression in bridges or buildings, estimating overall states with few sensors and implementing control), offering a reference for high-performance, low-cost active control systems.

Overall, Actuator angular displacement optimization model based on disturbance feedforward designs an optimal angular displacement trajectory based on the measurable disturbance hypothesis. While it effectively suppresses vibrations, it relies on idealized disturbance information and a precise system model, resulting in insufficient robustness. This limitation could be addressed by incorporating robust control or a disturbance observer to enhance adaptability. Extended state observer model based on acceleration measurements adopts an observer-based feedback control strategy using only acceleration measurements. Although innovative, it is susceptible to noise, and its control performance is compromised due to limited information. Future improvements could involve Kalman filtering to optimize estimation accuracy. A common drawback of both models is the oversimplified single-degree-of-freedom vehicle model and the reliance on a single performance metric. Enhancements would require developing a multi-degree-of-freedom model and conducting hardware-in-the-loop testing to improve feasibility and effectiveness in practical applications.

References

[1] Yi Qun, Li Caili. Research Status and Development Trends of Active Control Technology for Mechanical Vibrations[J]. Mechanical Engineering & Automation, 2016,(03):220-221.

[2] You Xiaoliang. Research on Key Technologies of Centrifugal Actuators for Active Vibration Control[D]. Nanjing University of Aeronautics and Astronautics, 2013.

[3] Hao Zhenyang, Wang Tao, Cao Xin, Gan Yuan, Yu Qiang. Modeling and Control of Rotating Eccentric Mass-based Damping Electric Actuator[J]. Journal of Vibration Engineering, 2022,35(01):209-219.

[4] Song Kuihui. Research on Rotor Hub Vibration Suppression Technology Based on Centrifugal Actuators [D]. Nanjing University of Aeronautics and Astronautics, 2021.

[5] Song Kuihui, Lu Yang, Cao Qingzhe. Experimental Investigation on Active Vibration Control of Rotor Hub Using Rotational Force Generators[J]. Journal of Vibration Engineering, 2022, 35(3):9.

[6] Hu Mingliang, Wang Lingwei, Chen Kui, et al. Research and Implementation of Centrifugal Actuator and Drive System [J]. Science Technology and Engineering, 2023, 23(6):2649-2655.

[7] Peng Bingshun, Zhang Chengtao. Research on Vehicle Lateral Control Algorithm Based on Linear Quadratic Regulator[J]. Automobile Parts, 2022,(10):17-20.

[8] Jung D. A Control Strategy of Actively Actuated Eccentric Mass System for Imbalance Rotor Vibration[J]. Actuators,2020,9(3):69.

[9] Zhang Weiwei. Systematic Study on Riccati Equation[J]. Journal of Anqing Normal University(Natural Science Edition), 2022(028-002).

[10] Xianping D, Chao S, Yiang Z, et al. Evaluation of vehicle vibration comfort using deep learning[J]. Measurement, 2020, 108634.